

Appendix A from N. Mideo et al., “Causes of Variation in Malaria Infection Dynamics: Insights from Theory and Data”

(Am. Nat., vol. 178, no. 6, p. 174)

Supplementary Methods

Effects of Experimental Manipulation

Some effects of our experimental manipulation of host immunity and RBC age structure can be seen in figure A1. Mean parasite densities for each treatment over the initial peak of infection are shown in figure A1, top row. As expected, parasite densities are higher in CD4⁺ T-depleted mice than in immune-intact control mice (Barclay et al. 2008). Mean RBC densities for each treatment over the initial peak of infection are shown in figure A1, bottom row. PHZ treatment results in a marked decrease in RBC densities. Figure A2 illustrates that PHZ-treated mice had significantly higher proportions of bloodstream reticulocytes and that a significantly higher proportion of infected RBCs were reticulocytes, across the relevant days postinfection.

Model Derivation

Basic Structure

Incorporating the age structure of the Mideo et al. (2008b) model into the model of Miller et al. (2010) yields the following basic model structure. On the $(i+1)$ th day postinfection, just after all infected red blood cells (RBCs) burst, the densities of merozoites, M_{i+1} , reticulocytes on their j th day in the bloodstream, $R_{j,i+1}$, and mature RBCs, N_{i+1} are given by

$$\begin{aligned}
 M_{i+1} &= \omega_R \sum_{j=1}^3 R_{j,i} [\lambda_R e^{(\lambda_R + d + I_{p,i})} + (1 - e^{-\lambda_R}) e^{-(d + d_2 + I_{p,i})}] \\
 &\quad + \omega_N N_i [\lambda_N e^{(\lambda_N + d + I_{p,i})} + (1 - e^{-\lambda_N}) e^{-(d + d_2 + I_{p,i})}], \\
 R_{1,i+1} &= [\theta(K - T_{i-\tau}) + dK] \frac{1 - e^{-(d + I_{u,i})}}{d + I_{u,i}}, \\
 R_{2,i+1} &= R_{1,i} e^{-(\lambda_R + d + I_{u,i})}, \\
 R_{3,i+1} &= R_{2,i} e^{-(\lambda_R + d + I_{u,i})}, \\
 N_{i+1} &= R_{3,i} e^{-(\lambda_R + d + I_{u,i})} + N_i e^{-(\lambda_N + d + I_{u,i})},
 \end{aligned}$$

where ω_R and ω_N are the number of progeny parasites produced in infected reticulocytes and mature RBCs, respectively, K is the normal total RBC density in the absence of infection and natural death, θ is the proportion of any RBC deficit that is made up in one day (and describes how RBC production increases with anemia; we therefore refer to it as the “upregulation rate”), d is the natural death rate of RBCs, d_2 is the additional death rate of multiply-parasitized RBCs and $T_{i-\tau} = \sum_{j=1}^3 R_{j,i-\tau} + N_{i-\tau}$ is the total RBC density τ days before i . The parameter τ allows RBC production in response to anemia to be time-lagged, since RBC precursors take time to develop in the bone marrow. The parameters $I_{p,i}$ and $I_{u,i}$ describe the immune clearance rates of parasitized and unparasitized RBCs as a function of time i . These parameters are described in more detail below. The parameters λ_R and λ_N define the average number of merozoites (that survive clearance in the bloodstream) per reticulocyte

and mature RBC, respectively. To find expressions for these parameters, we note that an individual merozoite has a probability of infecting a reticulocyte given by

$$\frac{\beta_R \sum_{j=1}^3 R_{j,i}}{\beta_R \sum_{j=1}^3 R_{j,i} + \beta_N N_i + \mu + I_{m,i}},$$

and an individual merozoite has a probability of infecting a mature RBC given by

$$\frac{\beta_N N_i}{\beta_R \sum_{j=1}^3 R_{j,i} + \beta_N N_i + \mu + I_{m,i}},$$

where β_R and β_N are the invasion rates of reticulocytes and mature RBCs, μ is the death rate of merozoites in the bloodstream, and $I_{m,i}$ describes the immune clearance rate of merozoites as a function of time, i . Multiplying these probabilities by the initial density of merozoites and dividing by the respective densities of RBCs gives the average number of merozoites per reticulocyte:

$$\lambda_R = \frac{\beta_R M_i}{\beta_R \sum_{j=1}^3 R_{j,i} + \beta_N N_i + \mu + I_{m,i}}$$

and the average number of merozoites per mature RBC

$$\lambda_N = \frac{\beta_N M_i}{\beta_R \sum_{j=1}^3 R_{j,i} + \beta_N N_i + \mu + I_{m,i}}.$$

The probability of a reticulocyte being infected by k merozoites is Poisson distributed with parameter λ_R and the probability of a mature RBC being infected by k merozoites is Poisson distributed with parameter λ_N (Miller et al. 2010). See Miller et al. (2010) for further details on the derivation of the model without age structure.

The model of Mideo et al. (2008b) discussed in the main text is recovered by setting all immune clearance parameters ($I_{m,i}$, $I_{p,i}$, and $I_{u,i}$) to 0. This is slightly different than the published model in Mideo et al. (2008b) since it tracks infections in time steps of thirds of a day rather than whole days and multiply infected RBCs are tracked separately. This allows the model to make predictions about the densities of unparasitized, singly parasitized, and multiply parasitized cells that should more accurately correspond to what is measured experimentally. However, all underlying biological hypotheses described by the model remain unchanged.

Immune Clearance

Three independent functions describe the immune clearance rates of merozoites, parasitized RBCs, and unparasitized RBCs over the course of infection (denoted $I_{m,i}$, $I_{p,i}$, and $I_{u,i}$). We assume that there are at maximum two ‘‘windows’’ of immune activity, and each window is described by four parameters (so each function is fully described by eight parameters). A schematic ‘‘clearance rate function’’ for parasitized RBCs is given in figure 1 of the main text. The parameter s_x defines the day postinfection when immune clearance begins, c_x represents the maximum clearance rate, r_x represents the time it takes to reach that maximum rate (or ‘‘rise time’’), and l_x represents the duration of immune clearance (note that $r_x \leq l_x$). The subscript x denotes the cells being cleared (either m for merozoites, p for parasitized RBCs, or u for unparasitized RBCs). For each immune clearance function, the two windows of immune activity will be described by a different set of parameters.

Model Fitting

The fitted model parameters and prior distributions are given in table A1. The prior distributions were either taken from the literature or based on our experimental measurements. The prior distributions for burst size, RBC upregulation rate, and invasion rate are specified with hyperparameters (table A2); hyperparameters essentially specify the distribution from which the individual-level parameters are randomly drawn. We do this for these parameters because we want to examine if they are parasite genotype-specific (see below).

As well as fitting the hybrid model (Mideo et al. 2008b; Miller et al. 2010) with age structure and immune responses, we fit a model without age structure (Miller et al. 2010) by setting reticulocyte and normocyte burst sizes and invasion rates equal ($\omega = \omega_N = \omega_R$, $\beta = \beta_N = \beta_R$) and a model without immune responses (Mideo et

al. 2008b) by setting immune-mediated clearance rates to 0 ($c_m = c_p = c_u = 0$). We also fit models without age structure and with each of the three immune components removed by setting their respective clearance rates to 0.

Miller et al. (2010) showed that there is a nonidentifiability between RBC invasion rate β and natural death rate of merozoites μ . This meant that it was impossible to obtain separate estimates for them and all that could be obtained was their ratio. In Mideo et al. (2008b), however, we did not fit μ but assumed it had a value of 48 d^{-1} ; thus, an estimate for β was obtainable. In order to test for genotype-specific differences in invasion rates we must therefore fix μ and assume that it is non-genotype-specific. Miller et al. (2010) estimated μ/β to be of the order 10^6 , taking $\mu = 48$ as in Mideo et al. (2008b) gives β^{-1} to be of the order 10^4 . The inverse of β is estimated rather than β because we have no prior knowledge about its upper bound.

In order to determine if there are genotype-specific differences in parameters we estimate the hyperparameters of the two strains in the model without age structure. For example, the prior distribution of burst size for AS-infected mice is $N(\nu_{\omega, \text{AS}}, \sigma_{\omega}^2)$ and for DK-infected mice $N(\nu_{\omega, \text{DK}}, \sigma_{\omega}^2)$. Terms $\nu_{\omega, \text{AS}}, \nu_{\omega, \text{DK}}, \sigma_{\omega}^2$ are hyperparameters that we estimate. If there are genotype specific differences in parameter estimates we expect to see a difference in the posterior distributions of $\nu_{\omega, \text{AS}}$ and $\nu_{\omega, \text{DK}}$, that is, the mean burst sizes of mice infected with AS and DK parasites, respectively. The variance hyperparameter σ_{ω}^2 is assumed to be non-strain-specific as it is of little interest here. We can also suppose that the burst sizes for all mice are randomly drawn from the same population, that is, non-strain-specific burst sizes, which means we take the prior as $N(\nu_{\omega}, \sigma_{\omega}^2)$ over all mice. We must also specify hyperpriors on the hyperparameters; these are given in table A2 and are chosen to be conjugate to the priors.

By estimating genotype-specific and non-genotype-specific hyperparameters we can calculate the (marginalized) likelihood ratio of the data supposing genotype-specific hyperparameters to the data supposing non-genotype-specific hyperparameters. Without any prior preference for these two suppositions their prior odds are 1 : 1. Thus, by Bayes's theorem, our posterior odds for these suppositions are equal to their likelihood ratio. If $\Pr(D_m|M)$ is the likelihood of mouse m 's data given model M , then our odds on genotype-specific hyperparameters is given by the ratio

$$\frac{\prod_m \Pr(D_m | \text{genotype-specific hyperparameters})}{\prod_m \Pr(D_m | \text{nongenotype-specific hyperparameters})}$$

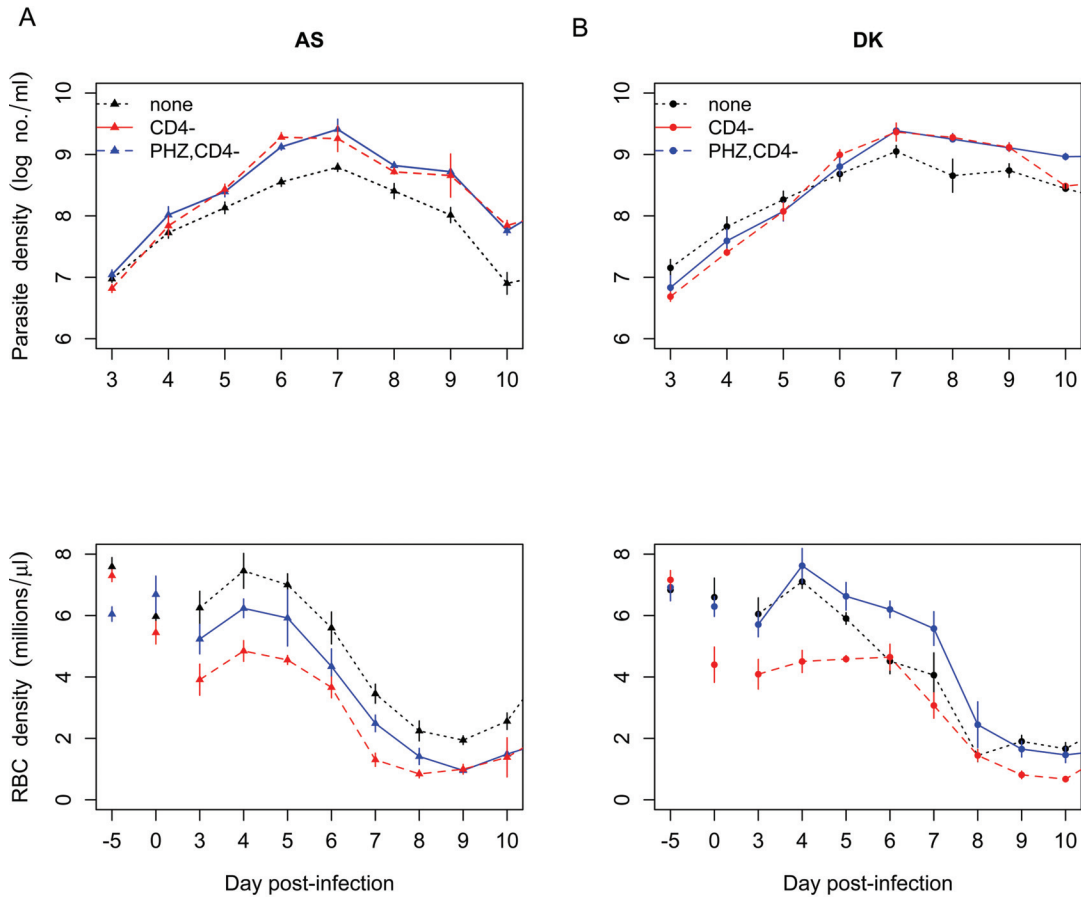


Figure A1: Infection dynamics of different treatments. Treatments are grouped by parasite genotype: *A*, More virulent parasite genotype AS; *B*, less virulent parasite genotype DK. Top row shows mean parasite density, and bottom row shows mean RBC densities over time. Error bars, ± 1 SEM. Colors indicate what treatments in addition to infection the hosts received: black, none (immune-intact control); blue, CD4⁺ depletion (CD4⁻); red, PHZ and CD4⁺ depletion. Over the course of the initial peak, parasite densities were higher in CD4⁺-depleted hosts as compared with immune-intact hosts. PHZ treatment (2 days before infection, i.e., day -2) resulted in a decrease in red blood cell densities. This effect coincided with the initial stages of infection.

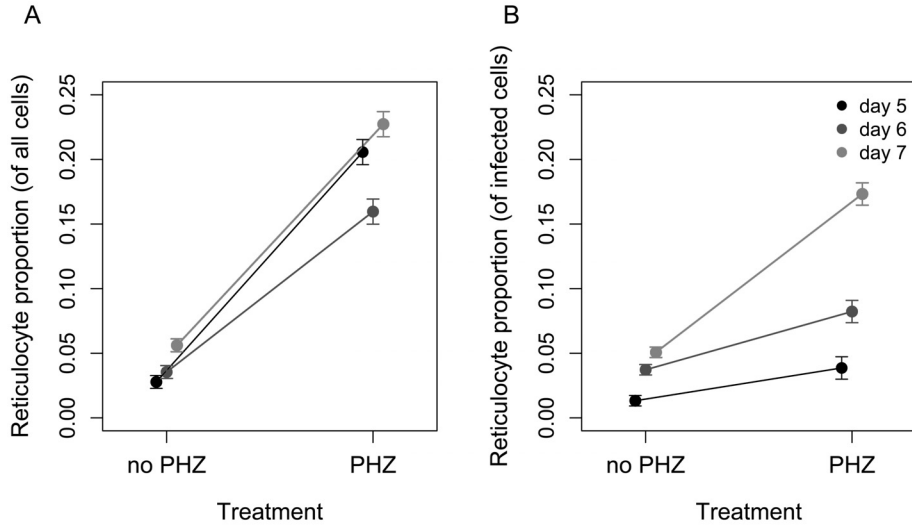


Figure A2: Effect of phenylhydrazine (PHZ) on red blood cell age structure in CD4⁺ depleted mice. The mean proportion of all red blood cells (RBCs) that are reticulocytes (A) and infected RBCs that are reticulocytes (B) over 3 consecutive days in untreated mice and those that received PHZ treatment. Error bars, ± 1 SEM. At the early stages of infection, mice treated with PHZ had a significantly higher proportion of reticulocytes, as expected, and subsequently, a significantly higher proportion of all infected cells were also reticulocytes.

Table A1. Model parameters and prior distributions of hybrid model

Parameter	Description	Value or prior	Source
ω_R, ω_N	Burst sizes in reticulocytes and normocytes	$N(\nu_\omega, \sigma_\omega^2)$	See table A2
β_R, β_N	Invasion rate of reticulocytes, normocytes ($[\text{cells}/\mu\text{L}]^{-1} \text{ s}^{-1}$)	Not fitted	
ρ	$\log_{10}(\beta_R/\beta_N)$	$N(0, .3^2)$	Hetzel and Anderson 1996; Antia et al. 2008; Mideo et al. 2008b
μ	Natural death rate of merozoites (day^{-1})	48	Garnham 1966; Mideo et al. 2008b
β^{-1}	Inverse of invasion rate (cells $s/\mu\text{L}$)	$\text{Exp}(1)$	See table A2
θ	Rate of upregulation of erythropoiesis (day^{-1})	$N(\nu_\theta, \sigma_\theta^2)$	See table A2
τ	Time lag in erythropoiesis (day)	$U(0, 6)$	Chang et al. 2004; Mideo et al. 2008b
d	Natural death rate of RBCs (day^{-1})	.025	van Putten 1958; Bannerman 1983
d_m	Increased death rate of multiply-parasitized RBCs (day^{-1})	$\text{Exp}(1)$	Miller et al. 2010
s_m, s_p, s_u	Start day of immunity targeting merozoites, parasitized RBCs, unparasitized RBCs	$U(0, 21)$	Miller et al. 2010
r_m, r_p, r_u	Rise time of immunity targeting merozoites, parasitized RBCs, unparasitized RBCs	$U(0, 21)$	Miller et al. 2010
c_m	Maximum level of immunity targeting merozoites (cells/s)	$\text{Exp}(10^8)$	Miller et al. 2010
c_p, c_u	Maximum clearance rate of immunity targeting parasitized RBCs, unparasitized RBCs (day^{-1})	$\text{Exp}(1)$	Miller et al. 2010
l_m, l_p, l_u	Duration of immunity targeting merozoites, parasitized RBCs, unparasitized RBCs	$U(0, 21)$	Miller et al. 2010
P_0	Initial parasite density (parasites/ μL)	$\log N(1.5, .5^2)$	Miller et al. 2010
N_0	Initial RBC density (RBCs/ μL)	$N_r(6.5 \times 10^6, 10^{12})$	

Note: RBC = red blood cell.

Table A2. Hyperparameters and their hyperprior distributions.

Hyperparameter	Description	Hyperprior	Source
ν_ω	Mean burst size	$N(6, .5^2)$	Garnham 1966; Carter and Walliker 1975; Carter and Diggs 1977; Mideo et al. 2008 <i>b</i>
σ_ω^2	Variance of burst size	$\text{InvGam}(2, 1^2)$	Garnham 1966; Carter and Walliker 1975; Carter and Diggs 1977; Mideo et al. 2008 <i>b</i>
ν_β	Mean inverse invasion rate	$\text{InvGam}(1, 10^4)$	Mideo et al. 2008 <i>b</i>
ν_θ	Mean red blood cell upregulation rate	$N(0.4, 0.2^2)$	Haydon et al. 2003; Mideo et al. 2008 <i>b</i>
σ_θ^2	Variance of red blood cell upregulation rate	$\text{InvGam}(2, 0.2^2)$	Haydon et al. 2003; Mideo et al. 2008 <i>b</i>